BMC Medical Genomics

RESEARCH

Open Access

Novel compound heterozygous *DOCK6* variants expand the mutational spectrum in prenatal diagnosis of Adams-Oliver syndrome 2

Xue Zhong[1,2], Xuan Zheng[3], Yinglei Xv[1,2], Kangxi Cai[4], Qianqian Wang[5] and Shiguo Liu[1,2*]

Abstract

Background Adams-Oliver syndrome (AOS) is a rare developmental disorder, and the *DOCK6* gene is an identified AOS gene. This report highlights the prenatal diagnosis of AOS-2 by ultrasonography and genetic testing.

Methods A growth-restricted fetus with bilateral ventriculomegaly, paraventricular calcifications, and ventricular septal defect underwent trio-whole-exome sequencing (trio-WES). Functional validation of the splice-altering variant was performed via minigene assays and protein structural modeling.

Results Trio-WES revealed compound heterozygous *DOCK6* variants: a paternal frameshift (c.3190_3191del; p.Leu1064Valfs60) and a maternal splice-site variant (c.3241-1G>T). Minigene assays demonstrated that c.3241-1G>T caused intron 26 retention (486 bp), introducing a premature termination codon (p.Val1081Glufs37). Structural modeling confirmed the loss of critical DHR2 domains in both truncated proteins.

Conclusions This study expands the mutational spectrum of *DOCK6* and underscores the importance of combining prenatal imaging with functional genomics for early diagnosis of AOS2.

Keywords *DOCK6*, Adams-Oliver syndrome 2, Minigene assay, Whole exome sequencing

Introduction

Adams-Oliver syndrome (AOS) (OMIM#614,219) is an autosomal recessive multiple congenital anomaly syndrome that is characterized by congenital cutaneous hypoplasia, terminal transverse limb defects, and variable involvement of the brain, eyes, and cardiovascular system(1). The clinical presentation of AOS is highly heterogeneous, with approximately 20% of patients with AOS suffering from congenital cardiac defects including atrial septal defects, ventricular septal defects, tetralogy of Fallot, as well as valvular abnormalities and ventricular anomalies(2). In contrast, neurological anomalies occur less frequently(3).

AOS-2 is caused by a homozygous or compound heterozygous pathogenic variant in the *DOCK6* gene, which

*Correspondence:
Shiguo Liu
liushiguo@qdu.edu.cn
[1] Medical Genetic Department, The Affiliated Hospital of Qingdao University, 16 Jiangsu Road, Qingdao 266003, China
[2] Prenatal Diagnosis Center, The Affiliated Hospital of Qingdao University, Qingdao, China
[3] Laboratory Medicine Department, Zhangdian People's Hospital, Qingdao, China
[4] Basic Medical College, Qingdao University, Qingdao, China
[5] Obstetrics Department, The Affiliated Hospital of Qingdao University, Qingdao, China

is located in the p13.2 region of chromosome 19 and encodes the DOCK6 protein, an atypical guanine nucleotide exchange factor that plays a role in cytoskeletal remodeling and neural protrusion growth(4).

This study describes a case of a fetus with an abnormal ultrasound that revealed the presence of novel compound heterozygous variants [c.3190_3191 del (p. Leu1064 Valfs*60) and c.3241-1G > T] in the *DOCK6* gene. To our knowledge, c.3241-1G > T is an unreported variant analyzed in detail to elucidate the complex genetic and phenotypic relationships of AOS-2, thereby improving the understanding of the spectrum of associated pathogenic variants.

Materials and Methods

Ultrasound examinations

The fetus was examined by ultrasound, including two-dimensional, Doppler, echocardiography, and fetal brain MR.

Trio-whole exome sequencing

The products of conception and peripheral blood (3 mL) of the parents were collected, and the whole genomic DNA was extracted by DNA extraction kit (TIANGEN China). DNA purity and concentration were determined using a Multiskan Go nucleic acid Protein analyzer (Thermo Fisher Scientific, USA). DNA with qualified concentration and purity was randomly interrupted into fragments ranging from 100 to 700 bp using a Covaris GS200 ultrasonic blocker, and the library was purified and screened using the Agcourt SPRIselect nucleic acid fragment purification and screening kit. The DNA library was subsequently subjected to PCR amplification and whole-exome capture using the Agilent Sure Select Human All Exon V6 kit. Illumina Nextseq500 sequencing system was used for sequencing. The 20 × coverage rate was 99.28% in the proband, 99.18% in his father, and 99.49% in his mother. Mutational pathogenicity ratings were performed based on the American College of Medical Genetics and Genomics (ACMG) guidelines and the ClinGen Sequence Variant Interpretation Expert Panel's recommendations for the application of the guideline criteria.

Bioinformatics analysis

SpliceAI Lookup (https://spliceailookup.broadinstitute.org/) was used to predict c.3241-1G > T impact. Use the SWISS-MODEL (https://swissmodel.expasy.org/) to build the DOCK6 protein before and after the mutation of the three-dimensional simulation diagram, using PyMOL 3.0.3 software amino acid variation before and after the analysis of the hydrogen bonds.

Minigene assay

The DOCK6 c.3241-1G > T variant is located in the last base of intron 26, which may affect splicing. To explore the effect of this variant on gene transcription, the wild-type DOCK6 target fragment (DOCK6 E(25–27)-F/R), including exon 25, exon 26, exon 27, and its intermediate intron (1039 bp), was amplified by PCR and verified by purification and sequencing. After purification and sequencing verification, the PCR product and linearised pEGFP-N1 expression vector were ligated by homologous recombination in EcoRI. The point mutation primers (DOCK6 c.3241-1G > T-F/R) were designed, and the candidate mutation point in the successfully constructed wild-type (WT) plasmid was mutated from G to A by Fast Mutagenesis System (Beijing Golden Biotechnology Co., LTD.). The successful construction of wild-type and mutant (MUT) minigene vectors was verified by transformation and PCR sequencing of bacterial fluid. 293 T cells were cultured with DMEM medium containing 10% fetal bovine serum in a 37℃ 5% CO2 incubator, and when the cells grew to 80% density, they were transfected according to the instructions of the Lipofectamine 3000 reagent (Thermo Fisher Scientific, USA), and cellular RNA was extracted after 24 h of incubation (TRizol extraction method). 1 μg of the total RNA was reverse transcribed into cDNA, and cDNA was subsequently amplified using the exon-specific primer on the plasmid (h-DOCK6 E25-27-F/R). PCR products were separated by 1% agarose gel electrophoresis and sequenced. The primers required for the Minigene experiments are listed in Table 1.

Results

Clinical manifestation of the abnormal fetus

A 24-year-old Chinese pregnant woman at 31-week gestation (WG) was referred to the Genetics Unit for an abnormal ultrasound examination. The couple were not consanguineous and denied relevant family history. Ultrasound in the preterm (II1) suggested a biparietal diameter of 7.17 cm, consistent with 28 weeks, 5 days; head circumference of 26.10 cm, consistent with 28 weeks, 3 days; transverse cerebellar diameter of 3.80 cm,

Table 1 Primer sequences for the Minigene assay

Primer names	Primer sequence
DOCK6 E(25–27) -F	agatctcgagctcaagcttcCAGGCACCTGTGTCCCCA
DOCK6 E(25–27) -R	taccgtcgactgcagaattcGCTAGACAGGAGCTC TGCTCA
DOCK6 c.3241-1G > T-F	ATTTTTCCCCCACTCTGCAtAGCTCCACCT
DOCK6 c.3241-1G > T-R	aTGCAGAGTGGGGGAAAAATGGGGGATGCC
h-*DOCK6* E25-27-F	GATGTGGAGCTGGCCGAG
h-*DOCK6* E25-27-R	GTTCGAGGGCCAGTGCCA

consistent with 31 weeks, 0 days; abdominal circumference of 23.51 cm, consistent with 27 weeks, 6 days; femur length of 5.45 cm, consistent with 28 weeks, 6 days; and humerus length of 4.81 cm, consistent with 28 weeks, 2 days. The body of the left lateral ventricle was about 1.09 cm wide. The posterior horn was about 0.74 cm wide, while the body of the right lateral ventricle was about 0.87 cm wide, and the posterior horn was about 0.96 cm wide (Fig. 1a); the medial walls of the bilateral lateral ventricles were not smooth, and multiple speckles of strong echogenicity were seen in the lateral walls and surrounding brain parenchyma (Fig. 1b). The continuity of the upper segment of the ventricular septum was interrupted, the width was about 0.23 cm, and the signal of blood flow through the septum was seen, which was a bidirectional low-velocity shunt (Fig. 1d). Fetal brain MR showed that the morphology of bilateral lateral fissure pools was irregular, bilateral ventricles were dilated and separated (Fig. 1e), with a width of about 11 mm at the widest point, and the corpus callosum was thinned, with part of the morphology not clearly shown (Fig. 1f).

Fetal ultrasound was performed again at 32-WG, still suggesting that the diameters were smaller than the week of gestation, with altered sonograms of the bilateral ventricular walls and brain parenchyma, ventricular septal defects and a corpus callosum that was approximately 3.02 cm long and 0.10 cm thick at the thinner part (Fig. 1c), with tortuous periportal arterial traveling. The parents decided to interrupt the pregnancy at 33-WG.

In this case, maternal serology screening for TORCH pathogens (IgM/IgG) was negative, and no other signs of congenital infection were detected.

Compound heterozygous variants of *DOCK6* causing fetal abnormalities

Trio-whole exome sequencing (Trio-WES) of aborted tissue showed a deletion variant exon26: c.3190_3191 del: p. L1064 Vfs*60 and a non-coding variant intron26: c.3241-1G > T in the fetal *DOCK6* gene (NM_020812.4). c.3190_3191 del was inherited from the father and c.3241-1G > T was inherited from the mother (Fig. 2a,b,c). According to the guidelines issued by ACMG, c.3190_3191 del: p. L1064 Vfs*60 was assessed as pathogenic (PVS1 + PS1 + PM2_Supporting), and c.3241-1G > T was assessed as pathogenic (PVS1 + PM3 + PM2_Supporting).

Bioinformatics analysis predicted that c.3241-1G > T would destroy the canonical splice acceptor site

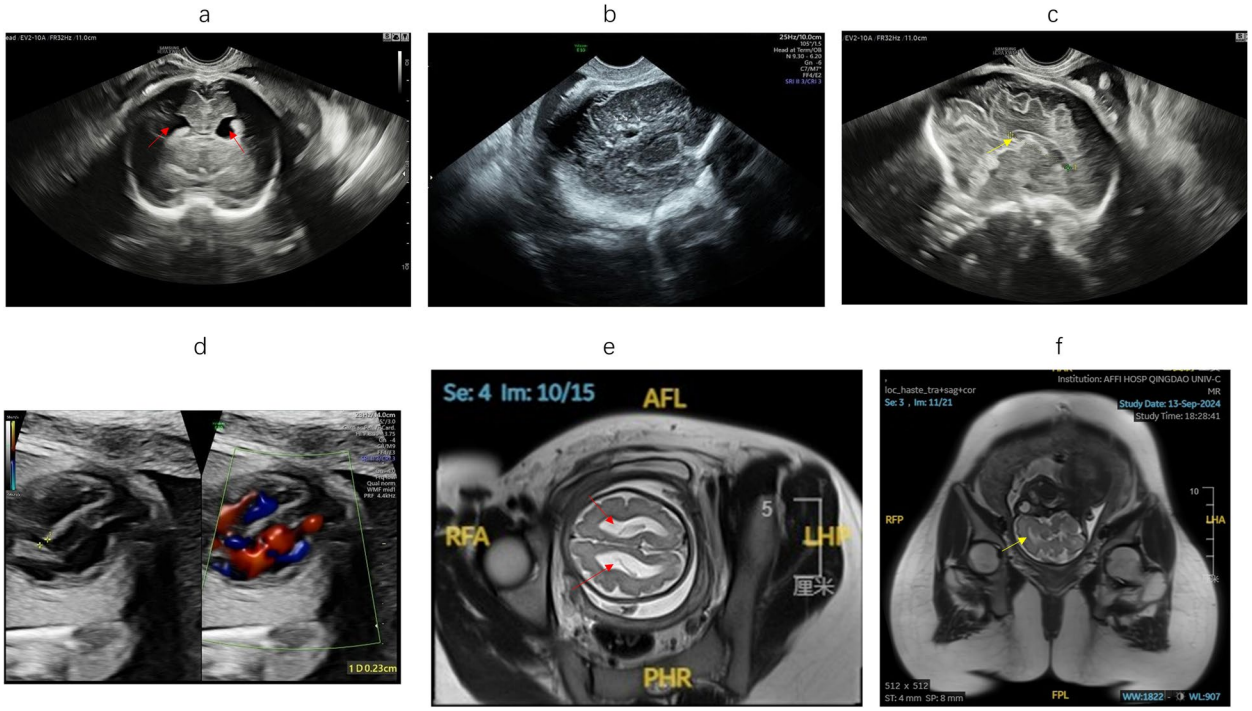

Fig. 1 **a**-**d** shows fetal ultrasound images at 31 or 32 weeks of gestation. **a** The ventricles were dilated bilaterally at 31 weeks of gestation. **b** The lateral walls of the bilateral ventricles were not smooth, and multiple speckles of hyperechogenicity were seen in the lateral wall and surrounding brain parenchyma at 31 weeks of gestation. **c** The corpus callosum was hypoplastic at 32 weeks of gestation. **d** Ventricular septal defect at 31 weeks of gestation. **e**–**f** is the MR Image at 31 weeks of gestation. **e** The fetal brain MR showed bilateral ventricular dilatation. **f** The corpus callosum was hypoplastic. (Red arrows indicate the location of ventricular expansion, yellow arrows indicate the location of the corpus callosum)

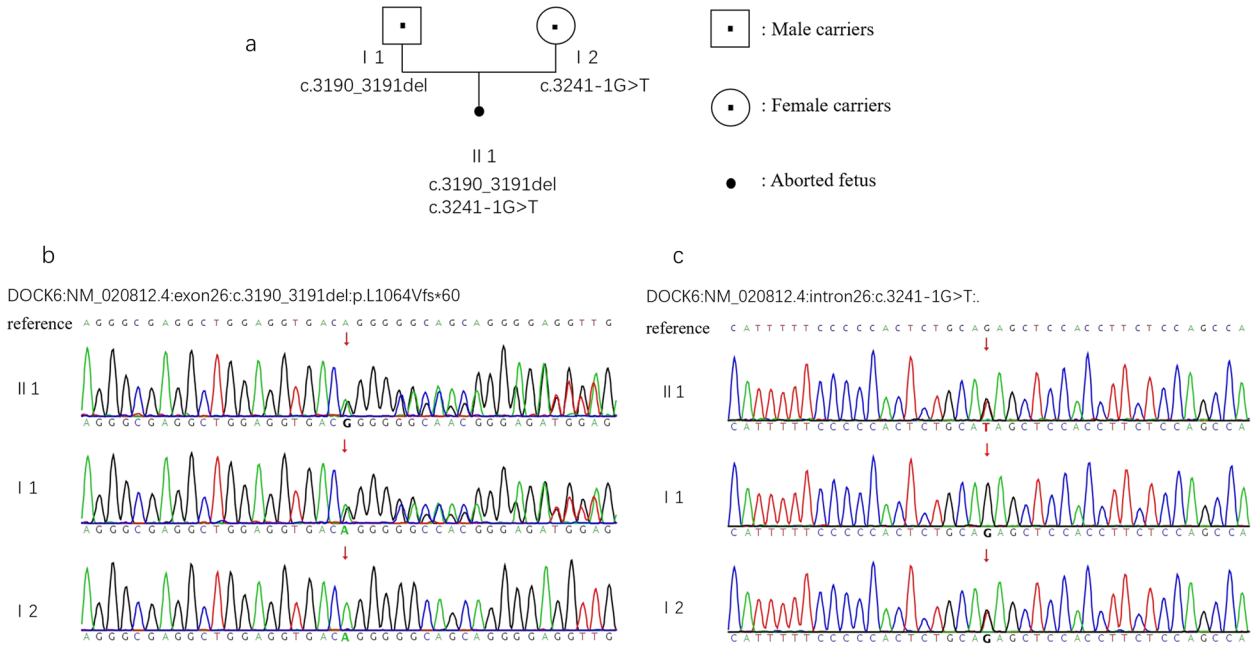

Fig. 2 Pedigree and sequencing chromatograms. **a** The pedigree of the family. **b** Sequencing chromatograms of the *DOCK6* c.3190_3191 del. **c** Sequencing chromatograms of the *DOCK6* c.3241-1G >T

(Δscore: 0.98). Three-dimensional representation of the DOCK6 protein, showing that the WT (normal) protein encodes 2047 amino acids and contains leucine at position 1064, whereas the deletion variant c.3190_3191 del protein contains valine at this position as well as terminating at 1124 amino acids and missing 924 amino acids. The non-coding variant c.3241-1G > T encodes only 1117 amino acids and is missing 930 amino acids compared to the WT. Both variant protein structures are significantly shorter than the WT protein (Fig. 3a, b).

Minigene assay confirmed that *DOCK6* variant c.3241-1G >T (NM_020812.4) affects mRNA splicing

WT and MUT recombinant plasmids were transfected into 293 T cells respectively, and cellular RNA was extracted for RT-PCR to detect the expression of WT and MUT *DOCK6* mRNA. Agarose gel electrophoresis results showed that the mutant group showed a larger amplified fragment compared to the WT group (Fig. 4a) (Full-length gels are presented in Supplementary Fig. 1). Sanger sequencing results further confirmed that the WT was a normal splicing band, and the MUT band resulted in an abnormal splicing result of the *DOCK6* gene mRNA (intron 26 stalled at 486 bp bases), which produced a termination codon in advance, and nonsense-mediated degradation of the mRNA level could occur (Fig. 4b,c).

Discussion

We used "Adams-Oliver syndrome 2" and "DOCK6" as qualifiers to collate cases with clear genotypes and phenotypes reported in PubMed, which were mostly diagnosed after genetic testing with clear clinical symptoms after birth, and fewer abnormalities were described in the prenatal stage. Fetal abnormalities observed in the antenatal stage so far include intrauterine growth restriction, oligohydramnios, fetal hypokinesis, cholestasis, meconium intestinal obstruction, and moderate ventricular dilatation with calcification (Table 2) (5–20). Fetal (II1) ultrasound suggested growth restriction, bilateral ventricular wall, brain parenchyma sonographic changes, paraventricular grey matter ectasia, a thin corpus callosum and ventricular septal defect (Table 3). Notably, the early-onset ventriculomegaly (detectable from 20 weeks) and calcification of ventricles may serve as a sentinel marker prompting DOCK6 analysis, particularly when coexisting with cardiac defects. A thin corpus callosum and ventricular septal defect emerge as novel prenatal markers, preceding classic postnatal scalp defects.

WES revealed the presence of both c.3190_3191 del (p.L1064 Vfs*60) and c.3241-1G > T variants of the *DOCK6* gene in the fetus. Both variants were rated as pathogenic according to the ACMG guidelines. One of them, c.3190_3191 del, is most frequent in clinical cases associated with AOS-2, resulting in the mutation of amino acid 1064 from leucine to valine and the generation of a new reading frame that terminates at codon 60 downstream

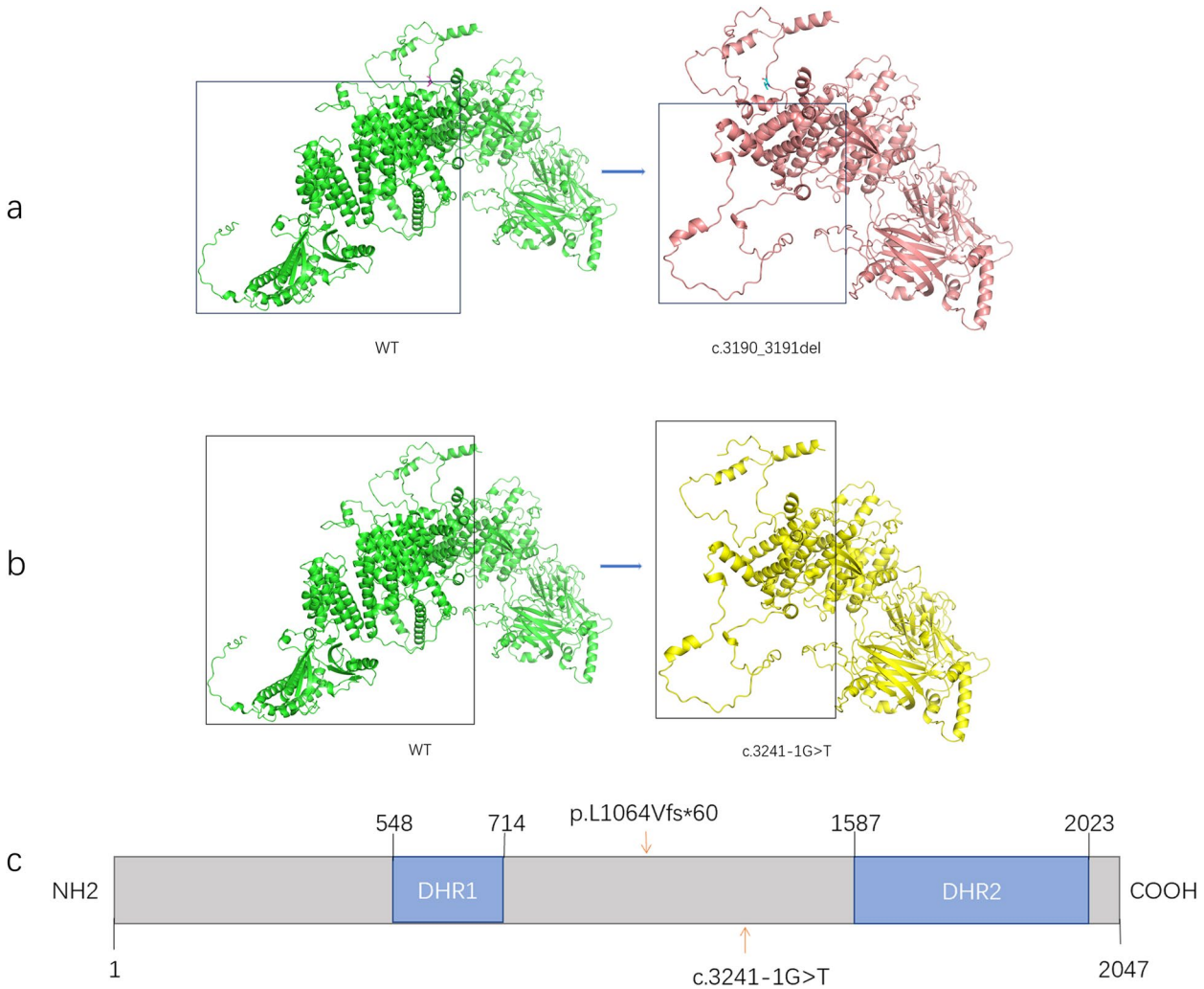

Fig. 3 Protein structure prediction. **a** Prediction of the 3D structure of DOCK6 protein before and after mutation (c.3190_3191 del) **b** Prediction of the 3D structure of DOCK6 protein before and after mutation (c.3241-1G >T) **c** DOCK6 protein pattern (arrows indicate the location of the mutation site)

of codon 1064. Another non-coding variant, c.3241-1G >T, which has not been reported in relevant clinical cases, is located in the last base of intron 26, presumably at the splice site. Searching the"DOCK6"gene in HGMD database(https://www.hgmd.cf.ac.uk/ac/index.php, Public version), a total of 44 known mutations were found, including 22 missense/nonsense mutations, 9 splicing mutations, 5 deletion mutations, 2 insertion mutations, 1 deletion insertion mutation and 1 complex rearrangement. Thus, 20% of reported *DOCK6* variants are splicing mutations, although previous studies have lacked mechanistic validation. Although computer simulation tools predicted that c.3241-1G >T would disrupt the typical splice acceptor site, functional validation is still essential considering that c.3241-1G >T is located at the most terminal 3'end of intron 26, where activation of the cryptic splice site could theoretically rescue normal splicing. Minigene results showed that the variant causes intron 26 of the DOCK6 gene mRNA to stall, resulting in a downstream shift (p. Val1081Glufs*37), confirming the pathogenicity of the variant locus. Minigene experiments enabled functional validation of the non-coding variant, overcoming the limitations of the WES-based prenatal assay, and eliminating endogenous gene confounders in regulation, confirming ACMG classification, and providing PS3/BS3 evidence for variant pathogenicity assessment.

The *DOCK6* gene encodes an atypical GEF that activates the Rho GTPase family members Cdc42 and Rac14, which are major regulators of cytoskeletal dynamics,

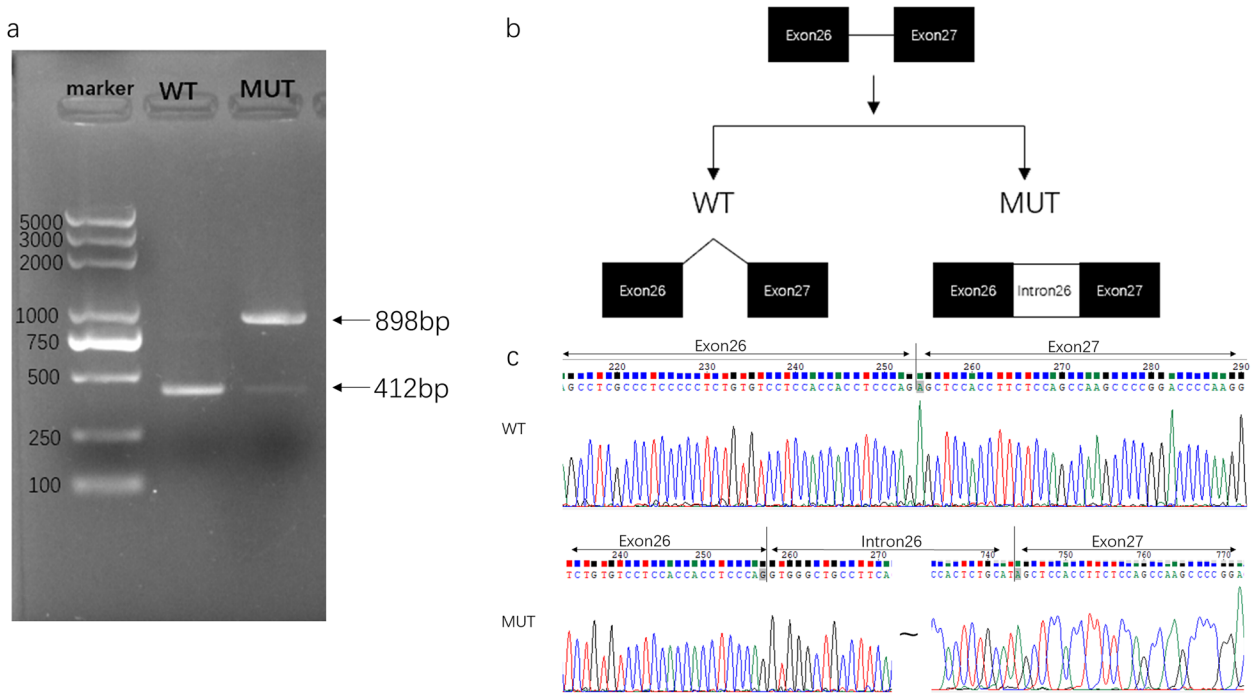

Fig. 4 Minigene assay. **a** Agarose gel electrophoresis of cDNA amplification, left for wild-type (WT) and right for mutant (MUT) **b** Schematic diagram of Minigene construction strategy and splicing. **c** Spliced bands correspond to sequencing result plots

directing key processes including neuronal migration, endothelial cell polarity and intracranial angiogenesis(1). After *DOCK6* gene mutation, the protein encoded by *DOCK6* is dysfunctional and cannot properly activate Cdc42 and Rac1, resulting in defects in the organization of the actin cytoskeleton, which will lead to abnormal cell behavior during embryonic development. During development, cells cannot normally migrate and differentiate, which may affect the development of the cardiovascular system and nervous system, leading to complications such as heart malformations and nervous system dysfunction. DOCK6 protein has two DOCK homology regions (DHR), namely DOCK homology region 1 (DHR-1), that encompasses amino acids 548 to 714, which is capable of binding phospholipids, and DOCK homology region 2 (DHR2), that encompasses amino acids 1587 ~2023, has guanine nucleotide exchange activity, specifically activates the Rho GTPases Cdc42 and Rac1(4). c.3190_3191 del and c.3241-1G > T resulted in the premature termination of the DOCK6 protein, both occurring before the DHR2 structural domain, and both proteins are predicted to have lost their normal function (Fig. 3c), which effectively eliminates GTPase binding/activating capacity, and the absence of Cdc42/Rac1 signaling impairs axon guidance and cortical plate compartmentalization, which could explain the fetal ventricular dilatation and paraventricular calcification, and defective endothelial cell skeleton remodeling may underlie septal defects and abnormal cerebral vasculature.

Ultrasound examination and genetic testing are complementary to each other in the diagnosis of AOS. Ultrasound examination focuses on the intuitive observation of the structure and function of the fetus and the patient and provides phenotypic information about the disease. Genetic testing can clarify the cause of disease from the molecular level and provide a key basis for diagnosis, treatment, and genetic counseling. The combination of the two methods can significantly improve the diagnostic accuracy and comprehensiveness of AOS and provide strong support for the management and treatment of patients.

Although our study extends AOS genotype versus phenotype, there are several limitations of our study that deserve consideration. First, although the aberrant splicing caused by c.3241-1G > T was confirmed by minigene assay. However, this in vitro system cannot fully replicate tissue-specific splicing regulation in vivo. Future studies using patient-derived induced pluripotent stem cells (iPSCs) differentiated into neuronal or cardiovascular lineages could better mimic tissue-specific splicing effects. Second, it is unknown whether the remaining N-terminal DHR-1 domain (aa548-714) exerts a dominant negative effect by interfering with wild-type DOCK6 or other DOCK family proteins.

Table 2 Genetic and clinical features of patients with Adams Oliver syndrome 2 by DOCK6 variants

Patient	Mutations	Consanguineous	Abnormalities in Pregnancy	Brain	Cardiovascular System	Scalp Defect	TTLD	Abnormalities of the Eye	Developmental Retardation	Reference
1	[c.4106 + 2 T > C] + [p. Y1021*]	-	na	Leukodystrophy, CCH	-	+	+	+	+	6
2	[p. Arg429GInfs*32] + [p. Arg429GInfs*32]	+	na	VD/BA	-	-	+	+	+	7
3	[p. Arg63Gln] + [p. Glu1792Lys]	-	na	VD/BA	na	+	+	na	+	8
4	[p. E1494*] + [c.5939 + 2 T > C]	-	IGR	PVL	PDA, PFO	+	+	na	na	9
5	[p. Thr455Serfs*24] + [p. Thr455Serfs*24]	+	na	VD/BA	-	+	+	+	+	1
6	[p. Asp416*] + [p. Asp416*]	+	Oligohydramnios and little fetal movement	-	-	+	+	-	na	1
7	[p. L1064 Vfs*60] + [c.4491 + 1G > T]	na	na	na	na	+	na	+	+	10
8	[p. L1064 Vfs*60] + [p. T48 Kfs*13]	-	na	CCH	na	-	na	+	+	11
9	[p. Glu1494 Ter] + [c.1105-1G > T]	-	IGR, cholestasis, and meconium ileus	na	VSD and PFO	+	+	na	+	12
10	[p. R466X] + [p. W1599X]	na	na	na	na	na	na	+	+	13
11	[p. Tyr835] + [c.5088 + 4 A > T]	na	Moderately dilated, calcified ventricles	VD/BA, CCH	na	+	+	na	+	14
12	[c.5939 + 2 T > C] + [deletion of exons 10 to 21]	na	na	PVL	na	-	+	+	na	15
13	[c.5939 + 2 T > C]+[deletion of exons 10 to 21]	na	na	na	na	na	na	+	na	15
14	[p. L1064 Vfs*60] +[p. E1494*]	-	Intrauterine restriction	na	TOF	+	+	+	+	16
15	[p. L1016P]+[p.L1016P]	+	na	na	na	+	+	+	+	5
16	[p. T455Sfs*24]+[c.4491 + 1G > A]	-	-	VD/BA, CCH	na	+	+	+	+	5
17	[p. Q434Rfs*21]+[p. Q434Rfs*21]	+	IGR	VD/BA, PVL	-	+	+	+	+	5
18	[p. R1596 W]+[p.R1596 W]	+	-	VD/BA	PDA	+	+	+	na	5
19	[p. F635Pfs*32] + [c.4106 + 5G > T]	-	-	+	-	+	+	+	+	5

Table 2 (continued)

Patient	Mutations	Consanguineous	Abnormalities in Pregnancy	Brain	Cardiovascular System	Scalp Defect	TTLD	Abnormalities of the Eye	Developmental Retardation	Reference
20	[p. F635Pfs*32] + [c.4106 + 5G > T]	-	IGR	na	Total Anomalous Pulmonary Venous Connection	-	+	+	+	5
21	[p. E162*] + [p. E162*]	+	na	na	na	+	+	na	na	5
22	[c.5235 + 205_6102-15 delins10] + [c.5235 + 205_6102-15 delins10]	+	-	PVL	na	+	+	na	na	5
23	[p. R841Sfs*6] + [p. R841Sfs*6]	+	-	VD/BA, CCH, PVL	na	+	+	na	na	5
24	[p. E1052 K] + [p.E1052 K]	+	IGR	VD/BA, CCH, PVL	-	+	+	+	+	5
25	[p. V263D] + [c.5939 + 2 T > C]	-	-	VD/BA, PVL	VSD	+	+	+	+	18
26	[p. V263D] + [c.5939 + 2 T > C]	-	IGR	VD/BA, CCH	na	+	+	+	na	18
27	[p. T455Sfs*24] + [p. T455Sfs*24]	+	na	VD/BA, PVL	-	+	+	+	+	19
28	[p.D416*] + [p.D416*]	+	na	na	-	+	+	-	+	19
29	[p. R841Sfs*6] + [p. R841Sfs*6]	+	na	VD/BA, PVL	Aortic valve dysplasia	+	+	-	na	20
30	[p. R841Sfs*6] + [p. R841Sfs*6]	+	na	VD/BA, PVL	na	+	+	na	na	20
31	[c.4107-1G > C] + [c.4107-1G > C]	+	na	PVL,pachygyria	na	+	+	+	na	20
32	[p. L1064 Vfs*60] + [p. E1494*]	-	IGR	PVL, porencephaly	TOF	+	+	+	+	21

Na no data available, *F* Female, *M* Male, *y* year(s), *m* month(s); *w* weeks(s); +,present; -,not present; VD/BA, ventricular dilatation/brain atrophy; CCH, corpus callosum hypoplasia/atrophy; PVL, periventricular lesions; VSD, ventricular septal defect; TOF, tetralogy of Fallot; PDA, patent ductus arteriosus; PFO, patent foramen ovale; IGR, Intrauterine growth retardation; TTLD, terminal transverse limb defect

Table 3 Fetal abnormal test results are associated with AOS

Method		Abnormal results
Ultrasound examination	Growth and development	growth restriction
	Nervous system	Ventricular dilatation
		Ventricular calcification
		Dysplastic corpus callosum
	Cardiovascular system	Ventricular septal defect
Genetic Testing	WES	DOCK6: c.3190_3191 del (p. L1064 Vfs*60), c.3241-1G > T

To address this issue, in vitro co-expression assays using truncated and full-length DOCK6, combined with Cdc42/Rac1 activation assays, could elucidate the mechanisms underlying dominant negativity or gain of function. Third, the prenatal markers proposed here, such as thin corpus callosum, need to be validated in a larger cohort. In addition, longitudinal studies tracing prenatal and postnatal phenotypes in genetically confirmed cases would help to determine the prognostic value of these ultrasound findings.

Conclusion

In this study, we identify a previously unreported compound heterozygous *DOCK6* mutation and confirm that the non-coding variant c.3241-1G > T can affect mRNA splicing and lead to AOS-2, which deepens the understanding of the *DOCK6* variant spectrum and helps to implement prenatal diagnosis of AOS-2.

Abbreviations

AOS	Adams-Oliver syndrome
ACMG	American College of Medical Genetics and Genomics
WT	Wild-type
MUT	Mutant
WG	Week gestation
Trio-WES	Trio-whole exome sequencing
DHR	DOCK homology regions

Supplementary Information

The online version contains supplementary material available at https://doi.org/10.1186/s12920-025-02157-w.

Additional file 1.

Acknowledgements

We thank the patients and their families for their participation.

Authors' contributions

XZ performed the experimental manipulations and wrote the manuscript of the paper. XZ analyzed and interpreted the data. YX performed the software operation and revised the manuscript. KC collected and entered the data. QW performed clinical data collection. SL conceived the study concept and design.

Funding

This research was funded by the National Natural Science Foundation of China grant number [30971586].

Data availability

The datasets generated and/or analyzed during the current study are available from the corresponding author upon reasonable request. The novel variant of DOCK6 revealed in the study has been submitted to ClinVar with the corresponding submission ID SUB15284669. https://submit.ncbi.nlm.nih.gov/subs/variation_clinvar/SUB15284669/. De-identified raw data can be made available upon reasonable request to the corresponding author of this study.

Declarations

Ethics approval and consent to participate

The study was conducted according to the guidelines of the Declaration of Helsinki and approved by the Ethics Committee of the Affiliated Hospital of Qingdao University (protocol code QYFY WZLL 27300 and date of approval 2025/2/20). All participants in this study provided written informed consent to participate.

Consent for publication

Participants provided written informed consent for clinical details as well as any identifying images to be published in this study.

Competing interests

The authors declare no competing interests.

Received: 24 February 2025 Accepted: 7 May 2025
Published online: 06 June 2025

References

1. Shaheen R, Faqeih E, Sunker A, Morsy H, Al-Sheddi T, Shamseldin HE, et al. Recessive mutations in DOCK6, encoding the guanidine nucleotide exchange factor DOCK6, lead to abnormal actin cytoskeleton organization and Adams-Oliver syndrome. Am J Hum Genet. 2011;89(2):328–33.
2. Meester JAN, Sukalo M, Schröder KC, Schanze D, Baynam G, Borck G, et al. Elucidating the genetic architecture of Adams-Oliver syndrome in a large European cohort. Hum Mutat. 2018;39(9):1246–61.
3. Digilio MC, Marino B, Baban A, Dallapiccola B. Cardiovascular malformations in Adams-Oliver syndrome. Am J Med Genet A. 2015;167a(5):1175–7.
4. Miyamoto Y, Yamauchi J, Sanbe A, Tanoue A. Dock6, a Dock-C subfamily guanine nucleotide exchanger, has the dual specificity for Rac1 and Cdc42 and regulates neurite outgrowth. Exp Cell Res. 2007;313(4):791–804.
5. Sukalo M, Tilsen F, Kayserili H, Müller D, Tüysüz B, Ruddy DM, et al. DOCK6 Mutations Are Responsible for a Distinct Autosomal-Recessive Variant of Adams-Oliver Syndrome Associated with Brain and Eye Anomalies. Hum Mutat. 2015;36(11):1112.
6. Wang Z, Wang X, Guiyu L, Litao Q, Shasha B, Tang X, et al. Novel compound heterozygous mutations of the DOCK6 gene in a familial case of Adams-Oliver syndrome 2. Gene. 2019;700:65–9.
7. Alzahem T, Alsalamah AK, Mura M, Alsulaiman SM. A novel variant in DOCK6 gene associated with Adams-Oliver syndrome type 2. Ophthalmic Genet. 2020;41(4):377–80.
8. Zhang K, Gao Z, Jin R, Lyu Y, Gao M, Gai Z, et al. Analysis of DOCK6 gene mutation in a child affected with Adams-Oliver syndrome type 2. Zhonghua Yi Xue Yi Chuan Xue Za Zhi. 2019;36(4):348–51.
9. Jones KM, Silfvast-Kaiser A, Leake DR, Diaz LZ, Levy ML. Adams-Oliver Syndrome Type 2 in Association with Compound Heterozygous DOCK6 Mutations. Pediatr Dermatol. 2017;34(5):e249–53.

10. Tao Z, Bu S, Lu F. Two AOS genes attributed to familial exudative vitreoretinopathy with microcephaly: Two case reports. Medicine (Baltimore). 2021;100(9):e24633.
11. Wu J, Lu AD, Zhang LP, Zuo YX, Jia YP. Study of clinical outcome and prognosis in pediatric core binding factor-acute myeloid leukemia. Zhonghua Xue Ye Xue Za Zhi. 2019;40(1):52–7.
12. Nieto-Benito LM, Suárez-Fernández R, Campos-Domínguez M. A novel pathogenic variation of DOCK6 gene: the genotype-phenotype correlation in Adams-Oliver syndrome. Mol Biol Rep. 2023;50(6):5519–21.
13. Jin EZ, Huang LZ, Zhao MW, Yin H. Atypical Adams-Oliver syndrome with typical ocular signs of familial exudative vitreoretinopathy. Int J Ophthalmol. 2022;15(8):1249–53.
14. Pisciotta L, Capra V, Accogli A, Giacomini T, Prato G, Tavares P, et al. Epileptic Encephalopathy in Adams-Oliver Syndrome Associated to a New DOCK6 Mutation: A Peculiar Behavioral Phenotype. Neuropediatrics. 2018;49(3):217–21.
15. Zepeda-Romero LC, Zenker M, Schanze D, Schanze I, Peña-Padilla C, Quezada-Salazar CA, et al. Intrafamilial phenotypic variability in autosomal recessive DOCK6-related Adams-Oliver syndrome. Eur J Med Genet. 2022;65(12):104653.
16. Lehman A, Stittrich AB, Glusman G, Zong Z, Li H, Eydoux P, et al. Diffuse angiopathy in Adams-Oliver syndrome associated with truncating DOCK6 mutations. Am J Med Genet A. 2014;164a(10):2656–62.
17. Brancati F, Garaci FG, Mingarelli R, Dallapiccola B. Abnormal neuronal migration defect in the severe variant subtype of Adams-Oliver syndrome. Am J Med Genet A. 2008;146a(12):1622–3.
18. Côté JF, Vuori K. Identification of an evolutionarily conserved superfamily of DOCK180-related proteins with guanine nucleotide exchange activity. J Cell Sci. 2002;115(Pt 24):4901–13.
19. Hassed SJ, Wiley GB, Wang S, Lee JY, Li S, Xu W, et al. RBPJ mutations identified in two families affected by Adams-Oliver syndrome. Am J Hum Genet. 2012;91(2):391–5.
20. Isrie M, Wuyts W, Van Esch H, Devriendt K. Isolated terminal limb reduction defects: extending the clinical spectrum of Adams-Oliver syndrome and ARHGAP31 mutations. Am J Med Genet A. 2014;164a(6):1576–9.

Publisher's Note